



Bulletin of the Mineral Research and Exploration

<http://bulletin.mta.gov.tr>



Comparison of the results of the suppression of surface related multiple reflections by predictive deconvolution in pre- and post-stack in 2D marine seismic reflection data: a case study from the Sea of Marmara

Mehmet Ali ÜGE^{a*} and Ali İsmet KANLI^a

^aIstanbul University-Cerrahpasa, Engineering Faculty, Department of Geophysical Engineering, Buyukcekmece, Istanbul, Türkiye

Research Article

Keywords:

Predictive Deconvolution, Seismic Reflection, Data Processing, Suppression of the Multiple Reflections, Marmara Sea.

ABSTRACT

This study aims to suppress the multiple reflections from the multi-channel seismic reflection data, which collected on the profile M97-29 at the Sea of Marmara with the MTA Sismik-1 Vessel in 1997 by the General Directorate of Mineral Research and Exploration (MTA), both at the pre- and post-stack stages separately, by using predictive deconvolution and to compare both results. The stack section obtained by applying predictive deconvolution to the pre-stack shot gathers, is compared with the stack section obtained by applying predictive deconvolution to the post-stack section, which has no predictive deconvolution application before stack. The multiple reflections are mostly suppressed in both sections, but the amplitudes of the primary reflections are much more noticeable and have much higher amplitudes on the stack section obtained by applying predictive deconvolution to the pre-stack shot gathers. Considering the data used in this study, which obtained from a shallow seabed section of the Sea of Marmara including sloped structures, it has been observed that the result obtained by applying the predictive deconvolution process to the pre-stack shot gathers are more successful than the other.

Received Date: 29.10.2020

Accepted Date: 30.06.2021

1. Introduction

The seismic reflection method is effective and widely used in many fields for exploration and development of oil and natural gas reserves, mapping hydrocarbon-containing formations and the surrounding geological structures, revealing complex geological structures containing fractures and faults under the seabed, and engineering studies. Converting the collected raw data, which have sufficient visual resolution for determination of underground geological structures in seismic reflection studies carried out onshore and offshore (sea and lake), to the seismic sections can be possible when the

collected data are as good as possible, and the processor has performed the seismic data-processing stages accurately and precisely. The sequence of data processes on seismic reflection data, application methods, and the choice of parameters may differ for each seismic data set. Increasing the signal/noise ratio of the seismic reflection data as a result of the applied data processing stages enables the next stage, the interpretation stage, to be performed both more easily and accurately.

In seismic reflection surveys, the energy emitted from the source after a shot can be subjected to more

Citation Info: Üge, M. A., Kanlı, A. İ. 2022. Comparison of the results of the suppression of surface related multiple reflections by predictive deconvolution in pre- and post-stack in 2D marine seismic reflection data: a case study from the Sea of Marmara. Bulletin of the Mineral Research and Exploration 167, 51-64.
<https://doi.org/10.19111/bulletinofmre.909820>

*Corresponding author: Mehmet Ali ÜGE, aliuge@istanbul.edu.tr

than one reflection before reaching the receivers. This special type of noise, which is called multiples, shows itself as multiple reflections in seismic sections and can cause difficulties during the interpretation stage. It is often a difficult process to distinguish the correct reflections from multiples at depth because the latter are recorded late on seismic sections. Especially in marine reflection seismic surveys, successive multiple reflections that are caused from seabed can mask and make the real (primary) reflections unrecognizable, which are below the recording time values observed in the cross-section. Therefore, failure to eliminate the effects of multiple reflections during data processing causes the interpreter to be unable to interpret properly or to make wrong interpretations during the interpretation stage.

Many different methods are used to suppress the multiple reflections observed in seismic reflection data. Predictive deconvolution is a special type of deconvolution, which is one of the most effective methods used to suppress the effects of multiple reflections over seismic sections. The predictive deconvolution is first introduced and applied to seismic data by Robinson (1957, 1967, 1975) then used by many different researchers on the data to suppress many different types of multiple reflections. Peacock and Treitel (1969) laid out the fundamental of the method and presented practical applications in suppression of multiple reflections in their studies. The theoretical development of predictive deconvolution from past to present could be found in the works of Verschuur (2013) and Weglein (1999) (Güney et al., 2019). Many authors had proposed new algorithms and application methods for the predictive deconvolution in order to suppress different types of multiple reflections (Taner, 1980; Taner and Coburn, 1981; Gibson and Lerner, 1984; Ulrych and Matsouka, 1991; Porsani and Ursin, 1998, 2007; Schoenberger and Houston, 1998; Perez and Hanley, 2000; Liu and Lu, 2008; 2014; Shankar et al., 2009; Margrave and Lamoreux, 2010; Wang et al., 2011; Güney et al., 2013; 2019).

The main purpose of deconvolution is to distinguish the reflectivity sequence from the seismic trace, thereby improving the vertical resolution and identifiability of the seismic events (Sheriff and Geldart, 1995). This method, which helps to eliminate the ringy appearance of seismic data, can also be applied to pre-stack shot gathers or Common Depth Point (CDP) gathers (deconvolution before stack - DBS) or deconvolution after stack (DAS).

However, the predictive deconvolution method plays an important role in increasing the spatial resolution in seismic reflection data.

The increase in spatial resolution provides important contributions and convenience in the stratigraphic interpretation of seismic reflection data, especially in thin layer analysis. The prediction lag and operator length parameters are important in the predictive deconvolution, so the selection of the values for these parameters should be made very carefully. In different survey areas, there were studies that have been carried out using the predictive deconvolution to suppress multiple reflections in marine seismic reflection data (Sinton et al., 1978; Marino et al., 2013; Sheng et al., 2014; Jian and Zhu, 2015; Bitencourt et al., 2017; Carneiro et al., 2017; Yuza et al., 2019).

When the preliminary studies previously carried out in the Marmara Sea are examined, it has been observed that the predictive deconvolution method does not give sufficient results and cannot be used effectively in suppressing the multiple reflections on the data where the seabed is shallow and has been found sloped structures (İmren et al., 2001; İmren, 2003; Düşünür, 2004; Yücesoy, 2006; Kurt and Yücesoy, 2009; Şapaş, 2010; Ergintav et al., 2011; Perinçek, 2011; Oğuz, 2012).

In this study, the multi-channel seismic reflection data collected on the line M97-29 (Figure 1) in the Marmara Sea by the MTA Seismic-1 Vessel in 1997 were obtained and the predictive deconvolution process applied separately both in the pre-and post-stack stages and the results are given comparatively. The results are presented about, at what stage multiple reflections can be suppressed more accurately by the predictive deconvolution for these data obtained from the Sea of Marmara.

2. Methods

Multi-channel marine seismic reflection data used for suppression of multiple reflections by using the method of predictive deconvolution were collected by MTA in 1997 in the Marmara Sea with the MTA Seismic-1 Vessel (Figure 1). The data acquisition parameters of the seismic line M97-29 selected for this study are shown in Table 1. The shot record, taken from the midpoint of the M97-29 seismic line where primary and multiple reflections can be seen, is presented in Figure 2.

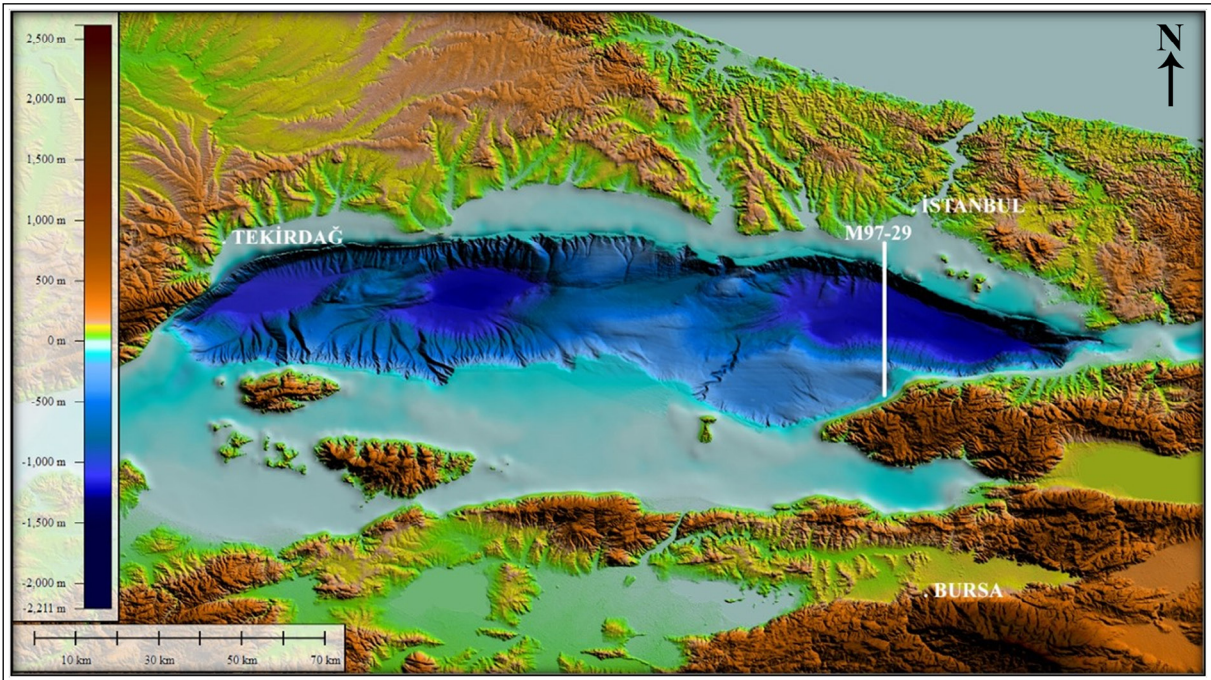


Figure 1- The location map of seismic data collected by MTA in 1997 with the MTA Seismic-1 Vessel in the Marmara Sea and showing the location of the line to which the data used in this study belong.

Table 1- Data acquisition parameters of M97-29 seismic line.

Seismic Line	Source	Channel Number	Shot Interval	Receiver Interval	Offset	Record Length	Sampling Rate	Fold
M97-29	Air-gun	84	50 m	12.5 m	40 m	6 s	2 ms	11

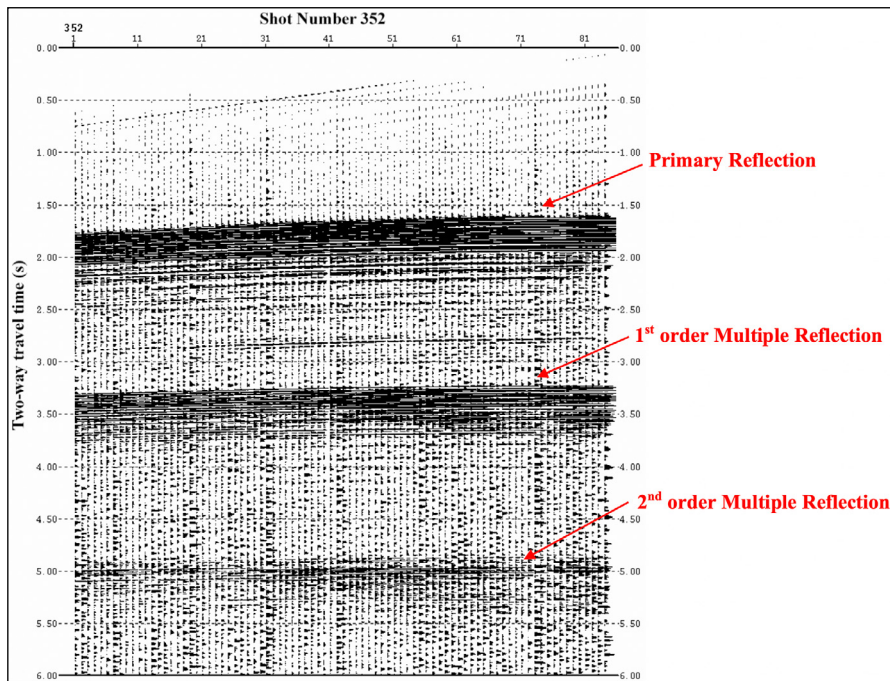


Figure 2- Shot number 352, taken from the midpoint of the M97-29 seismic line and the observed primary and multiple reflections in this shot record.

2.1. The Predictive Deconvolution

The predictive deconvolution process must be carried out very carefully because if it is applied incorrectly to the seismic data, it can significantly affect the information of real (primary) seismic reflections, causing the high-frequency noise present in the data to increase and the amplitude of the primary reflections to decrease. This situation may cause seismic sections to be misinterpreted by the interpreter during the interpretation stage.

The predictive deconvolution is performed by using parameters predicted from the autocorrelation of the seismic signal (the prediction lag and the operator length). The prediction lag is an important parameter for the predictive deconvolution process. Choosing the prediction lag correctly ensures that the spatial resolution in the data is increased and its multiple reflections in the data are suppressed. If the prediction lag is chosen close to the sampling rate, the resolution of the seismic data will be increased, while if a larger value is chosen, the multiple reflections in the seismic data will be suppressed. The other important parameter of the predictive deconvolution process is the operator length. The operator length is expressed as the time-domain length of the part where the autocorrelation of the seismic trace is approximately equal to the wavelet autocorrelation (Dondurur, 2018). If the operator length has not been selected at sufficient or has been selected a low value, the suppressing process of the multiple reflections on the data cannot be performed properly.

Figure 3 shows the autocorrelation section of a trace from the seismic reflection data. This autocorrelation signal was used to determine the values of the parameters (the prediction lag and the operator length) of the predictive deconvolution process to be applied to the seismic data.

In the seismic reflection data including long-path multiples, the predictive deconvolution process performed by choosing the prediction lag equal to the value of the multiples period (the time value for the trace of multiple reflections observed in the autocorrelation section) will provide the most appropriate results. The optimal results can be obtained if the operator length is selected as the value of the time covered by the multiple reflections in the seismic trace autocorrelation section (Dondurur, 2018).

The predictive deconvolution method can also be applied to the pre-stack shot gathers or the CDP gathers or the post-stack sections. When applying the predictive deconvolution before the stack, the chosen prediction lag values for the shot or the CDP gathers vary depending on the offset (Dondurur, 2018). When applying the predictive deconvolution after the stack, the prediction lag values to be selected for the stack sections do not change depending on the offset due to the Normal Move Out (NMO) correction. The parameters to be selected for the predictive deconvolution process are selected by looking at the autocorrelation section of each shot or CDP gather before the stack. Moreover, the parameters to be selected for the predictive deconvolution process after the stack, are selected by giving the seabed points marked on the stack section to the system and looking

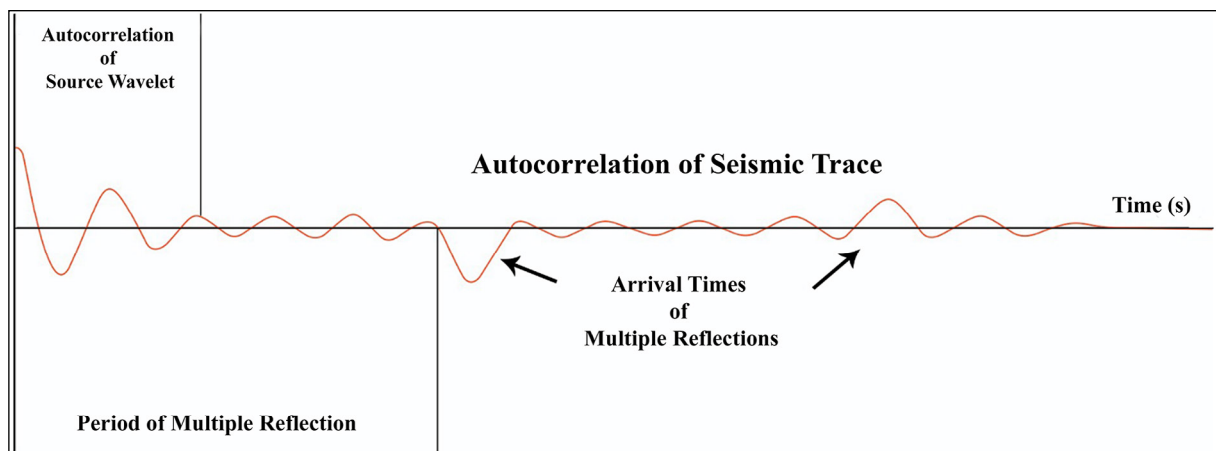


Figure 3- The multiple reflections on the autocorrelation section (modified from Dondurur, 2018).

at the autocorrelation of the traces found at these points.

3. Findings

In this study, the results obtained from the pre-and post-stack stages separately, by using the predictive deconvolution to the multi-channel seismic reflection data collected on the line numbered M97-29 in the Marmara Sea with the MTA Seismic-1 Vessel in 1997 are given comparatively. Thus, interpretations were made about the stage at which the multiple reflections observed in seismic data can be suppressed more effectively by using the predictive deconvolution. Data processing sequence of this work is presented in Figure 4.

3.1. The Application of the Predictive Deconvolution to the Pre-Stack Shot Gathers

Within the scope of the study, first of all, it was ensured that the multiple reflections observed in

the data were suppressed by applying a predictive deconvolution method to the shot gathers in which the shot and receiver geometries were defined in the system. The optimum prediction lag and the operator length values were determined by autocorrelation analysis in order to perform the predictive deconvolution process. For the application of pre-stack, this process was made from the auto-correlation section of one-shot gather in every 10 shot gathers. If more frequently the parameter selections are made in the application of predictive deconvolution, the success of the application will be higher. The shot gather 352 taken from the middle part of the seismic line can be seen in Figure 2. In this record, it is seen that the primary reflections are approximately at 1.6 s, the 1st multiple reflections are approximately at 3.2 s, and the 2nd multiple reflections are at approximately 4.8 s.

In Figure 5a, the auto-correlation section of the shot gathers 352 and the auto-correlation trace for

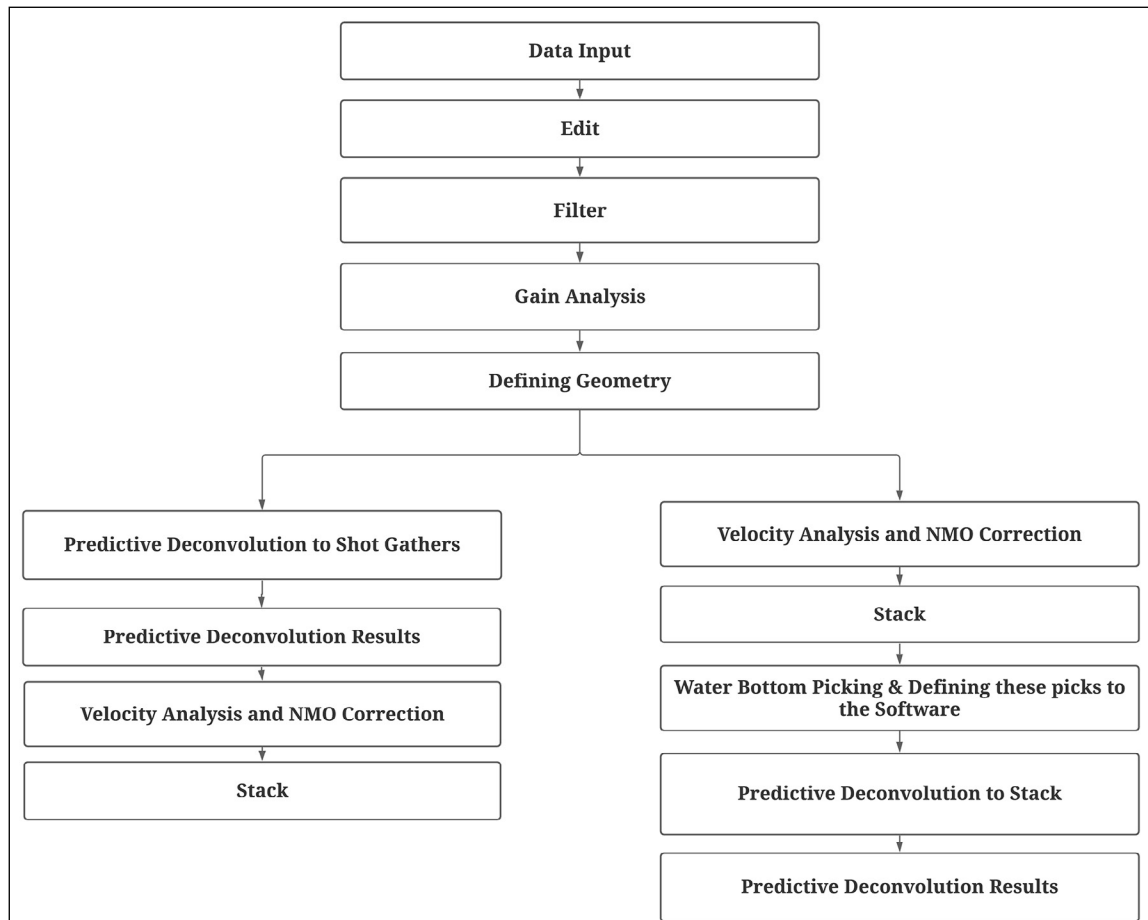


Figure 4- The sequence of data processing for the seismic reflection data.

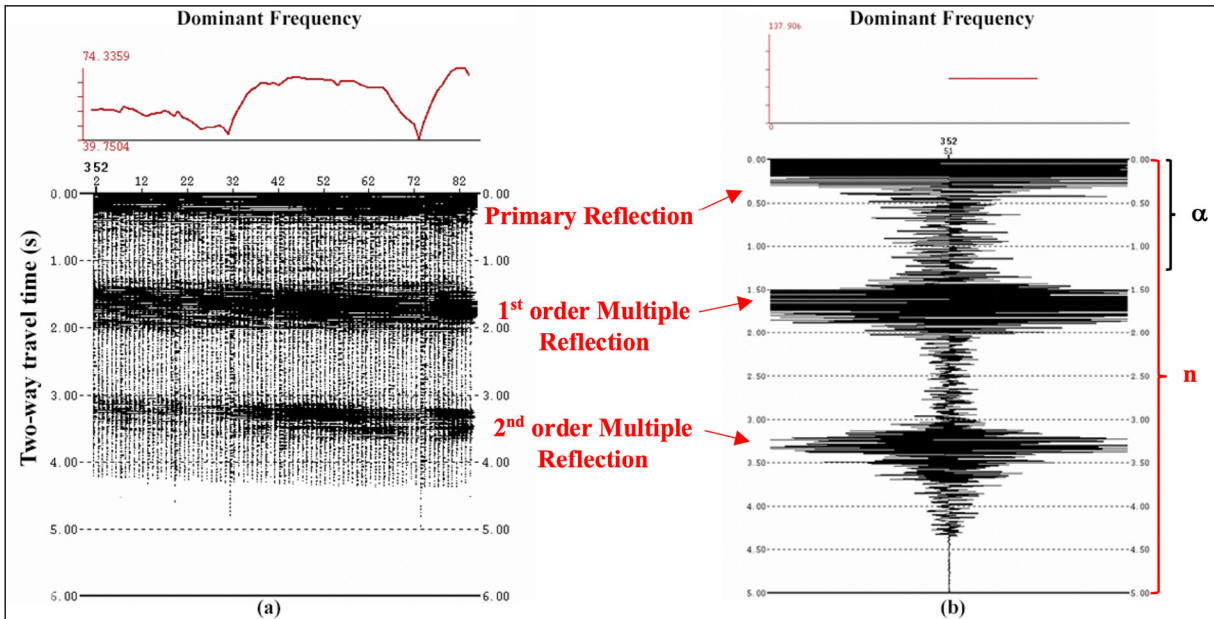


Figure 5- a) The auto-correlation section for the shot gather 352 and b) the auto-correlation section for trace 51 of the shot gather 352.

trace 51 of the shot gather 352 is seen in Figure 5b. In the predictive deconvolution process, choosing the prediction lag (α) value equal to the period of the multiple reflection that will be seen first in the auto-correlation section and choosing the operator length (n) value to include the multiple reflections in the auto-correlation section will be effective in suppressing the determined multiples.

As a result of the parameter tests, the most suitable prediction lag value for the shot gather 352 was determined as 1250 ms and the most suitable operator length value was determined as 5000 ms. As a result of the tests using different values, it was observed that the multiple reflections could not be suppressed sufficiently, and the signal/noise ratio of data was affected negatively (Figure 6).

If the prediction lag is chosen equal to the period value of the first multiple reflections observed in the autocorrelation section, the predictive deconvolution process gives a suitable result, and apart from this, the multiple reflections observed in the shot gather could not be suppressed. If the operator length value is selected as a time value that includes multiple reflections observed in the auto-correlation section of the shot gather, the predictive deconvolution process yielded an appropriate result, and apart from this, the multiple reflections observed in the shot gather could not be suppressed with the values used. For comparison,

the shot record 352 and the Fourier amplitude spectrum of this record are given in Figure 7a, and the shot record after the predictive deconvolution and the Fourier amplitude spectrum of this record are given in Figure 7b. As a result of the predictive deconvolution process, the multiple reflections were suppressed and the distorting effects of the multiple reflections on the data were eliminated. These distorting effects removed from the data are also observed in the Fourier amplitude spectrum comparisons given in Figure 7a and Figure 7b. The disturbing effects of multiple reflections covering the primary reflection amplitudes in the Fourier amplitude spectrum were eliminated after the predictive deconvolution process. After the predictive deconvolution process was completed, stack section obtained from applying the velocity analysis and NMO correction in accordance with the given workflow (Figure 4) is given in Figure 8.

3.2. The Application of Predictive Deconvolution After Stack

As the next step within the scope of the study, as indicated in the workflow in Figure 4, the stack section was obtained by applying processing steps except for predictive deconvolution (Figure 9), and the multiple reflections were suppressed by applying the predictive deconvolution to this stack section. Since the stack section is always zero offsets, the processing step of the predictive deconvolution before the stack and the

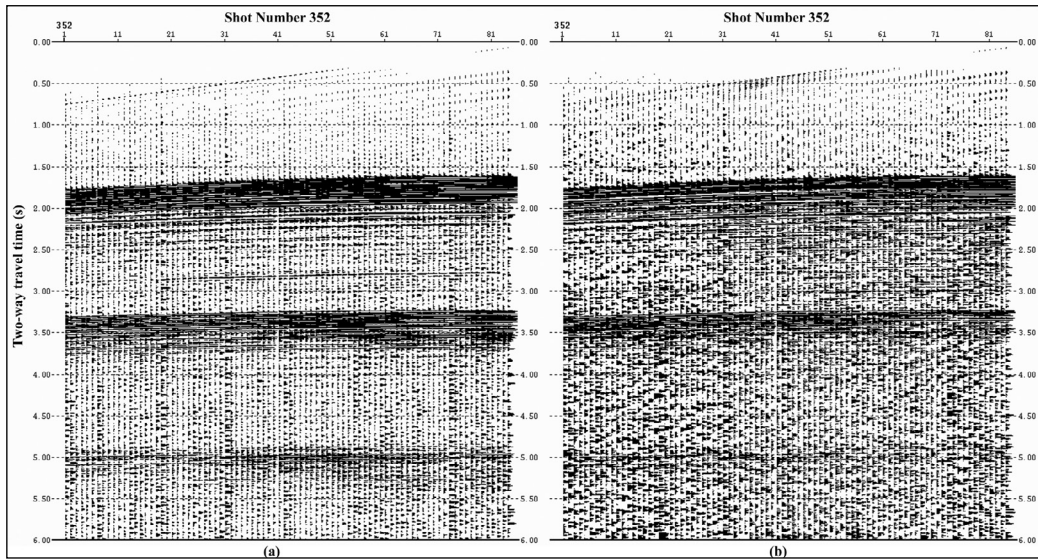


Figure 6- a) The record for the shot gather 352, and b) the result of the predictive deconvolution using the prediction lag $\alpha = 7$ ms, the operator length $n = 1200$ ms.

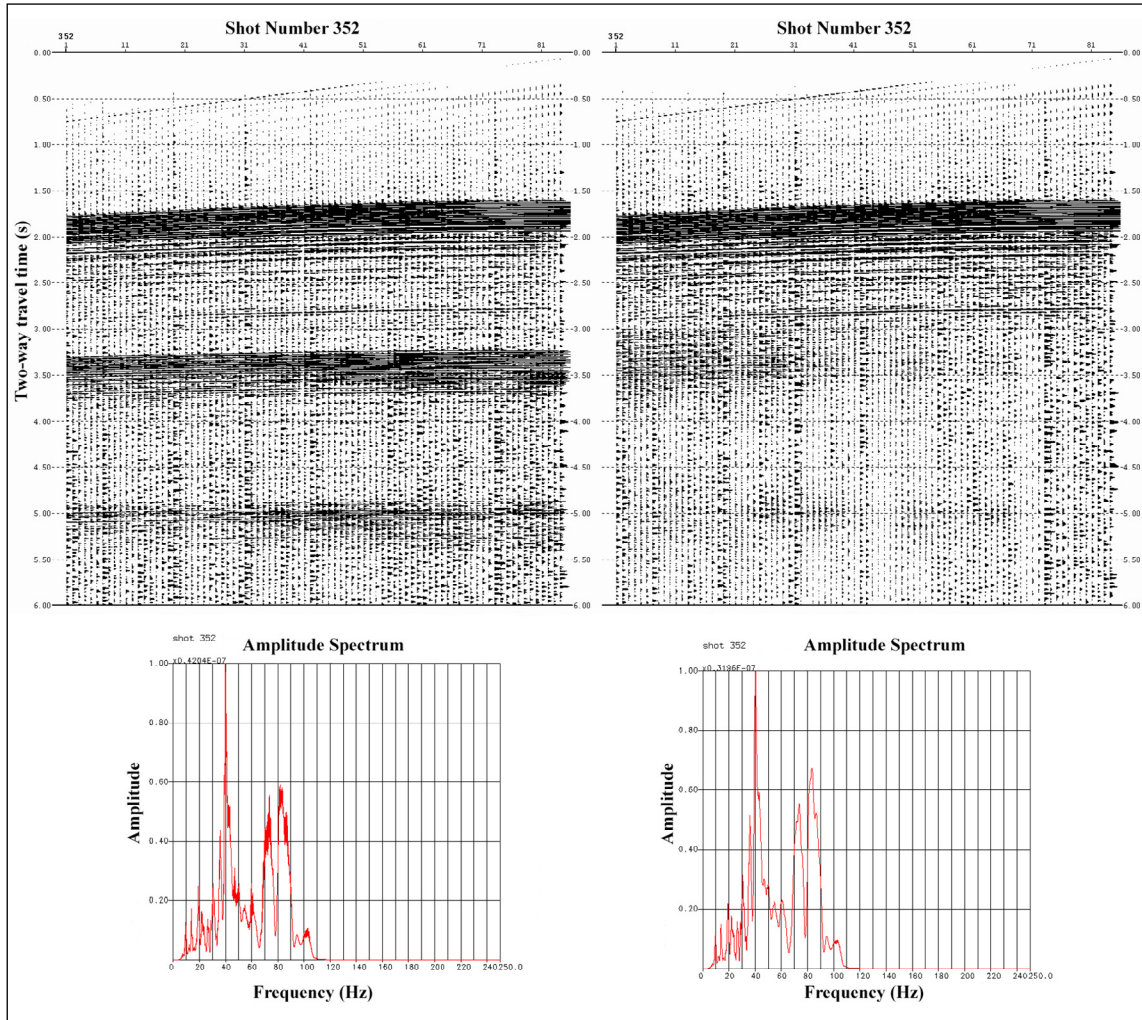


Figure 7- The record for shot gather 352 (upper left) and its Fourier amplitude spectrum (lower left), the result of the predictive deconvolution using the prediction lag $\alpha = 1250$ msec and the operator length $n = 5000$ msec (upper right) and its Fourier amplitude spectrum (lower right).

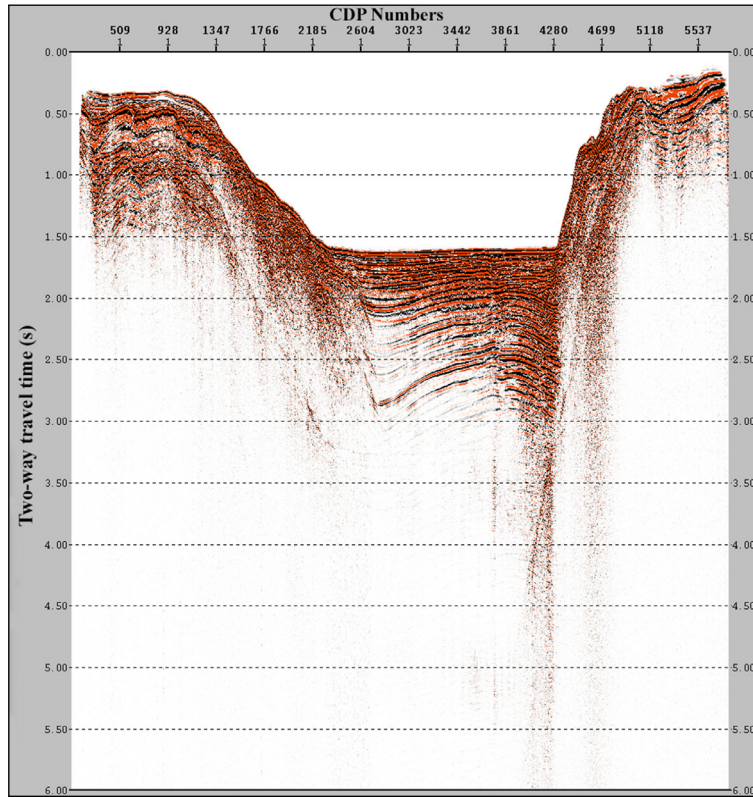


Figure 8- The stack section obtained by applying the predictive deconvolution before stack.

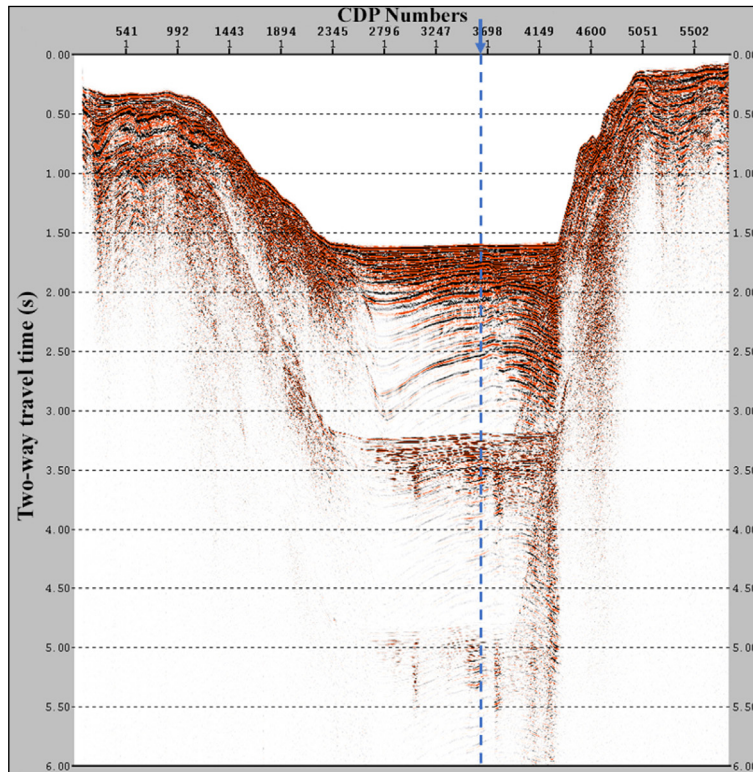


Figure 9- The stack section obtained from the data process flow is indicated in Figure 4. The blue dashed line (indicates the location of selected the CDP trace 3641 for the parameter selection). Especially, the seabed reflection between the CDPs 2345 - 4200 is approximately 1.6 s in the cross-section, and its multiple reflections are clearly seen at 3.2 s.

processing step of the predictive deconvolution after the stack show differences. The main difference is that the prediction lag value changes depending on the offset in the application of predictive deconvolution before stack, while the prediction lag values do not vary depending on the offset in the post-stack application due to the zero offset.

In the application of predictive deconvolution after stack, the seabed level above the stack section is marked (Figure 10, green dashed line) and the parameters are determined by calculating the auto-correlation of the traces starting from this level. There will be differences in the determined predictive deconvolution parameters due to the differences in the time of arrival of primary and multiple reflections on the section, where the seabed is not stable in the stack section.

For the cases where the seafloor remains relatively flat, it is sufficient to determine the prediction lag and operator length values by analyzing the autocorrelation trace of a CDP trace (blue dashed vertical line in Figure 9 and Figure 10), while for the cases where the seabed changes sharply, the prediction lag and operator length values are determined by analyzing the auto-correlation sections of the several CDP traces.

Figure 11a shows the auto-correlation section of the whole stack section, and Figure 11b shows the auto-correlation trace of the CDP trace no 3641 selected on the section. In addition, the prediction distance (α) and operator length (n) values selected for the predictive deconvolution stage to be applied to the CDP trace 3641 are shown on Figure 11b.

As a result of many different parameter tests performed on the CDP trace 3641, the most suitable prediction lag value was determined as 1300 ms and the most suitable operator length value was determined as 4000 ms. As a result of tests using different values, it was observed that multiple reflections could not be suppressed sufficiently. However, it has been observed that the most ideal results are obtained when a time value is chosen, where the prediction lag is equal to the first multiple reflection period values observed in the auto-correlation section, and the operator length is a time value that includes the multiple reflections observed in the auto-correlation section. Figure 12a shows the stack section obtained without applying the predictive deconvolution and the average Fourier amplitude spectrum of this stack section, Figure 12b shows the stack section obtained from the application of predictive deconvolution after the stack and the average Fourier amplitude spectrum of this stack

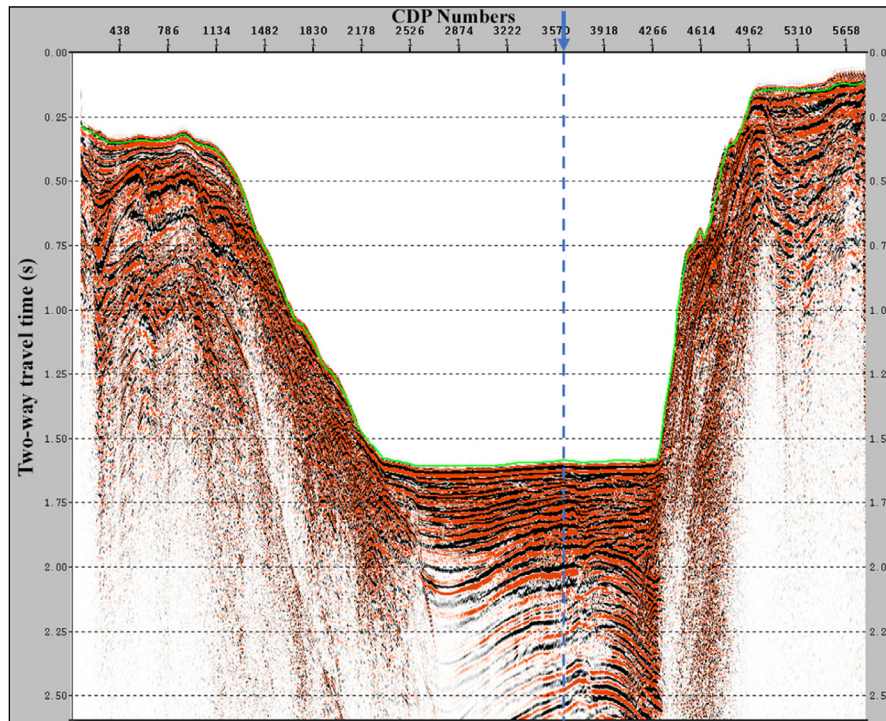


Figure 10- Marking the seabed above the stack section (green continuous line) in order to giving the changing seabed depth values to the system.

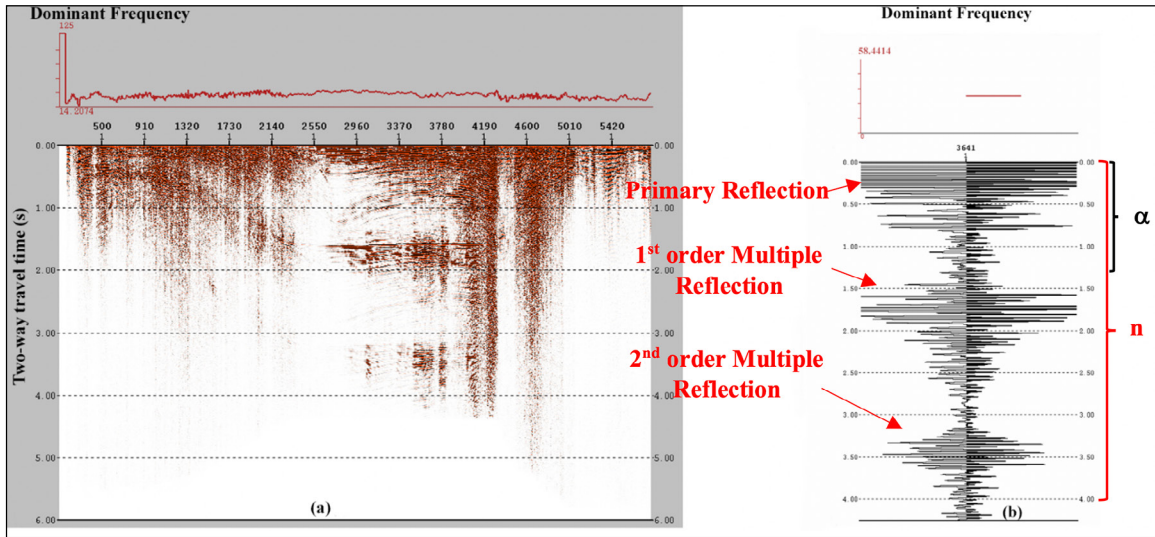


Figure 11- a) The auto-correlation section for the whole section of the stack and b) the auto-correlation section belonging to the CDP trace 3641 selected on the section.

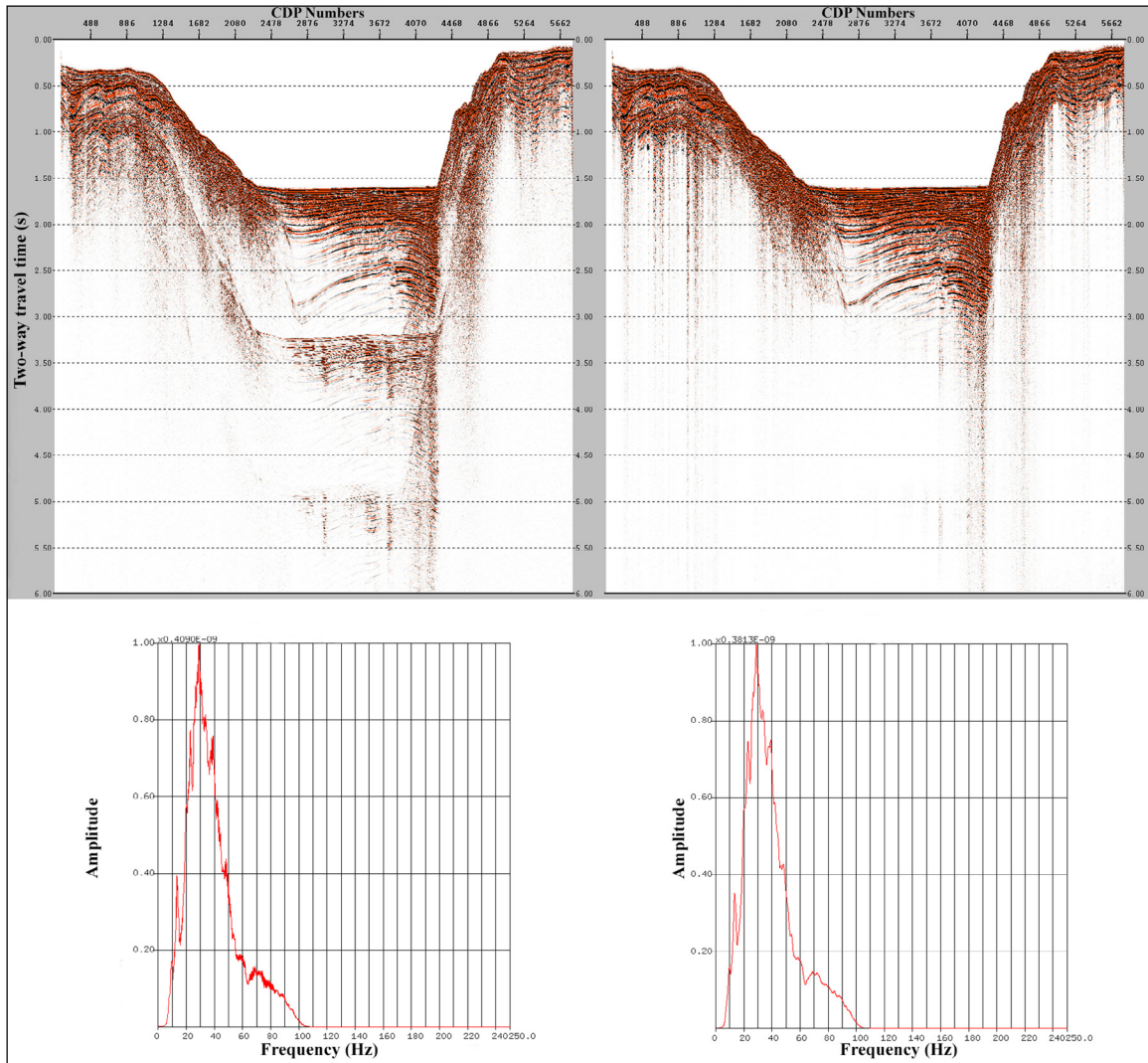


Figure 12- The stack section obtained without applying the predictive deconvolution (upper left) and the Fourier amplitude spectrum belonging to this section (lower left), the section obtained by applying the predictive deconvolution to the stack section (upper right) and the Fourier amplitude spectrum belonging to this section (lower right).

section. When the Fourier amplitude spectrum in Figures 12a and 12b were compared, it was observed that the effects of multiple reflections on the primary reflection amplitudes were removed as a result of the predictive deconvolution after the stack stage, but it was observed that the primary reflections on the section were lost by reducing the maximum amplitude value.

4. Results

In this study, the result obtained by applying the predictive deconvolution to the pre-stack shot gathers and the result obtained by applying the predictive deconvolution to the stack section obtained without applying the predictive deconvolution to the shot gathers (deconvolution after stack) were compared. The optimal prediction lag and operator length values for both applications were determined by making many tests.

Determining the prediction lag and operator length values in the most appropriate way is very important for the effective application of the predictive deconvolution process. However, choosing the prediction lag equals to the period of the multiple reflections, and choosing the operator length as the value of the time covered by the multiple reflections increases the quality of the applied predictive deconvolution process.

When the results obtained with the application of predictive deconvolution to pre-stack shot gathers are examined, it is observed that the multiple reflections on the shot gathers are largely suppressed. As seen in the example given for the 352 shot gather in Figure 7b, the multiple reflections were suppressed and the amplitudes of the primary reflections in the 15 - 20, 30 - 40, 80 - 90 Hz intervals in the Fourier amplitude spectrum increased.

After the predictive deconvolution process is carried out, there is an increase in the amplitudes of the noises observed in the shot gathers. For this reason, a band-pass filter based on cut-off frequencies of 5 - 10 / 110 - 120 Hz was applied to the sections after the predictive deconvolution process, and the signal/noise ratio of the sections are increased.

When the results obtained from the predictive deconvolution after stack are examined, it is seen that the multiple reflections observed in the section are mostly suppressed, but they are negatively affected in the amplitudes of the primary reflections (Figure 12b).

The Fourier amplitude spectrum of stack section obtained from applying the predictive deconvolution to the pre-stack shot gathers in Figure 13a and the Fourier amplitude spectrum of stack section obtained from applying the predictive deconvolution to the post-stack section in Figure 13b, are given. As a

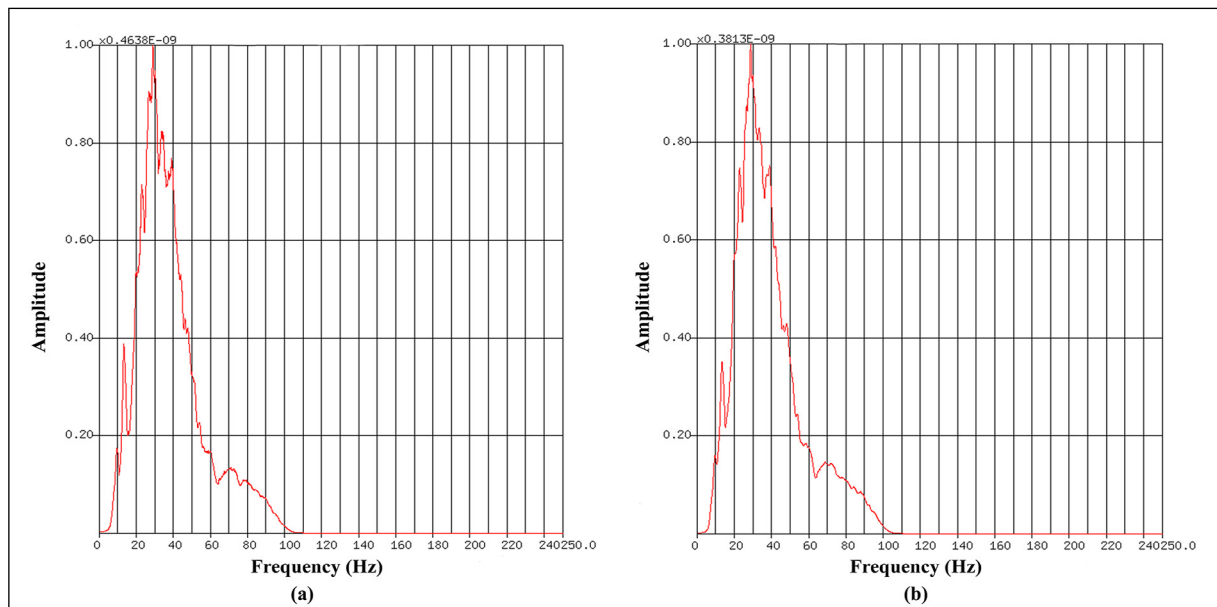


Figure 13- a) The Fourier amplitude spectrum of the stack section obtained as a result of the applied predictive deconvolution before stack and b) the Fourier amplitude spectrum of the stack section obtained as a result of applied the predictive deconvolution after stack.

result of the comparison, the highest amplitude value of the section is $0,4638^{-9}$ in Figure 13a, while the highest amplitude value of the section is $0,3813^{-9}$ in Figure 13b. The predictive deconvolution increases the spatial resolution in seismic reflection data and provides important contributions and convenience in the stratigraphic interpretation of seismic reflection data, especially in thin layer analysis. Considering this situation, in Figure 14, the differences of primary reflection amplitudes are revealed as a result of the

comparison of the stack sections obtained with the pre- and post-stack processing steps specified in the workflow in Figure 4.

The stack sections obtained with the pre-and post-stack processing steps specified in the workflow in Figure 4 between CDPs 2300 and 4210 and 1.60-3.40 s, are applied by Automatic Gain Control (AGC), are shown in Figures 14a and 14b. The sections, between 4.20 - 5.80 s at the same CDP intervals, are

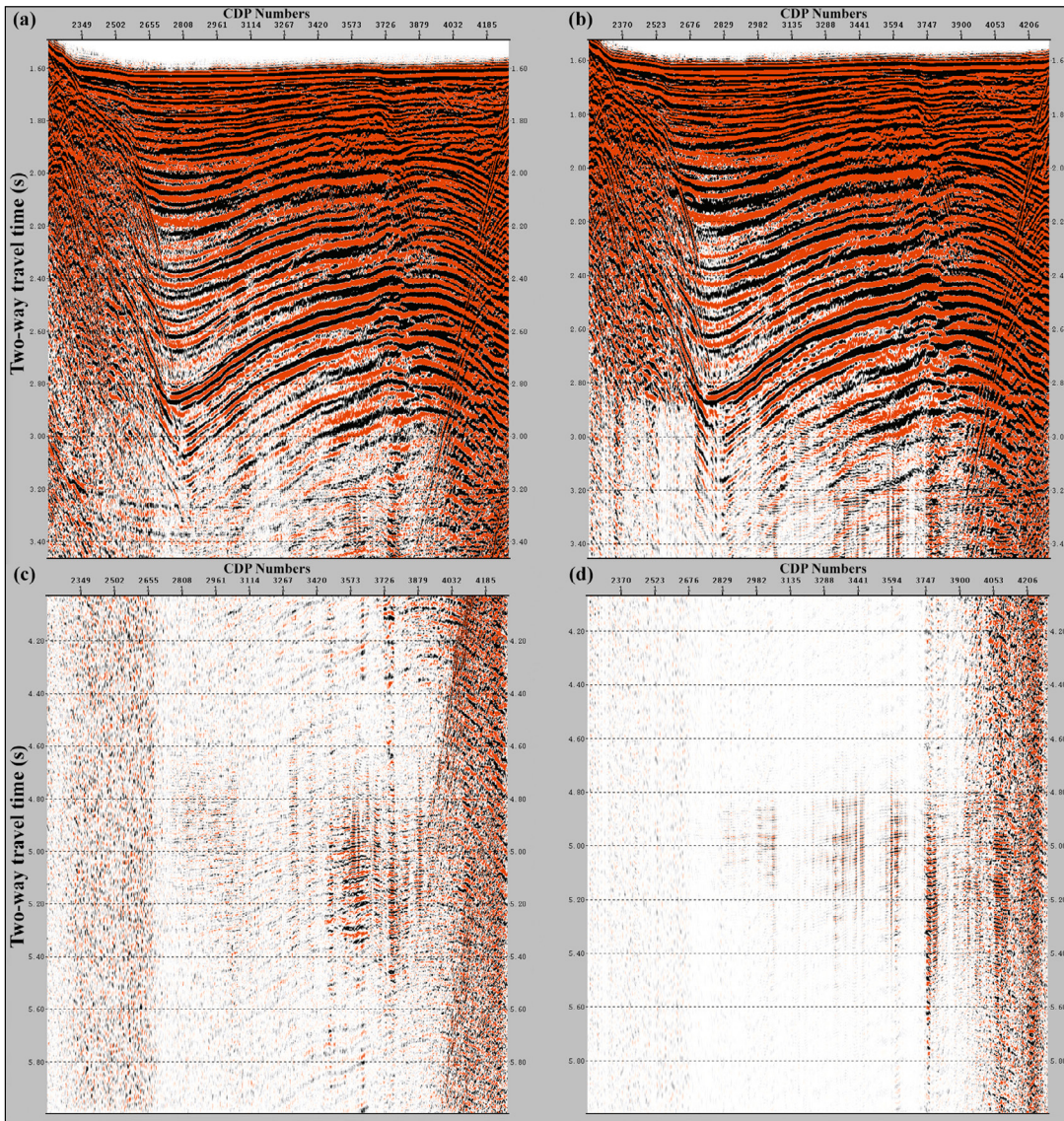


Figure 14- a) The stack section obtained by applying the predictive deconvolution to the pre-stack shot gathers, where the AGC is applied to the part between 2300 and 4210 CDPs and between 1.60 - 3.40 s, b) the stack section obtained by applying the predictive deconvolution to the post-stack section, where the AGC is applied to the same CDP and time intervals, c) the stack section obtained by applying the predictive deconvolution to the pre-stack shot gathers, where the AGC is applied to the part between 2300 and 4210 CDPs and between 4.20 - 5.80 s, and d) the stack section obtained by applying the predictive deconvolution to the post-stack section, where the AGC is applied to the same CDP and time intervals.

applied by AGC, which can be seen in Figures 14c and 14d. When the relevant figures are compared, it is observed that the identifiability of the amplitudes of the primary reflections in Figure 14b and Figure 14d have decreased according to the amplitudes in Figure 14a and Figure 14c (especially in the deeper sections).

When the pre-and post-stack sections were compared by the following workflow in Figure 4, it is clearly seen that the multiple reflections in both sections are largely suppressed, but the primary reflection levels are much more selectable and the high quality with pre-stack processes compared to post-stack processes. As a result, considering the data of the seismic line number M97-29 collected in the Marmara Sea used in this study, it was observed that the results obtained by applying the predictive deconvolution to the pre-stack shot gathers were more successful than the others.

Acknowledgments

We would like to thank The Directorate of Mineral Research and Exploration for providing the multichannel seismic reflection data collected in the Marmara Sea within the scope of this study with the decision dated 23.10.2019 and numbered 85699071 - 105.02 - E.79352 and the staff of the MTA Seismic Vessel 1 and the reviewers who spent their valuable time helping to improve the whole article. Moreover, we thank Emerson & Paradigm Inc. for the Paradigm GeoDepth software that it provided to the university with an education license. This study was supported by Istanbul University Cerrahpaşa, Scientific Research Projects Coordination Unit with the project coded FDK - 2020 - 34714. This study includes a part of Mehmet Ali UGE's PhD thesis named Application of Seismic Migration methods to Marmara Sea Reflection Data and Interpretation of Active Tectonics.

References

- Bitencourt, L. S., Castro, H. B. S., Fontes, P. H. L., Silva, M. G., Porsani, M. J. 2017. Singular value decomposition and multichannel predictive deconvolution applied to multiple attenuations of Jequitinhonha basin. 15th International Congress of the Brazilian Geophysical Society and EXPOGEF, 31 July - 03 August 2017, Rio de Janeiro, Brazil, 612-615.
- Carneiro, R. N. C., Leite, L. W. B., Vieira, W. W. S., Rufino, C. S. 2017. Predictive deconvolution of multiple free surfaces in marine seismic data. 15th International Congress of the Brazilian Geophysical Society and EXPOGEF, 31 July - 03 August 2017, Rio de Janeiro, Brazil, 598-602.
- Dondurur, D. 2018. Acquisition and Processing of Marine Seismic Data. Elsevier, 606.
- Düşünür, D. 2004. Orta Marmara Havzası'nın aktif tektonik yapısının deniz jeofiziği akustik yöntemleriyle araştırılması, Yüksek Lisans Tezi, İstanbul Teknik Üniversitesi, Fen Bilimleri Enstitüsü, 127 (unpublished).
- Ergintav, S., Demirbağ, E., Ediger, V., Saatçılar, R., İnan, S., Cankurtaranlar, A., Dikbaş and A., Baş, M. 2011. The structural framework of onshore and offshore Avcılar, Istanbul under the influence of the North Anatolian Fault. *Geophysical Journal International* 185(1), 93-105.
- Gibson, B., Larner, K. 1984. Predictive deconvolution and the zero-phase source. *Geophysics* 49(4), 379-397.
- Güney, R., Karşlı, H., Dondurur, D. 2013. Ofset bağımlı önkestirim dekonvolüsyonu. *Jeofizik* 17, 3-12.
- Güney, R., Karşlı, H., Dondurur, D. 2019. Optimum parameter selection in offset-dependent predictive deconvolution: testing on multichannel marine seismic data. *Marine Geophysical Research* 40, 601-617.
- İmren, C. 2003. Marmara Denizi faal tektonizmasının sismik yansıma verileri ile incelenmesi. Doktora Tezi, İstanbul Teknik Üniversitesi, Fen Bilimleri Enstitüsü, 203 (unpublished).
- İmren, C., Le Pichon, X., Rangin, C., Demirbağ, E., Ecevitoglu, B., Görür, N. 2001. The North Anatolian Fault within the Sea of Marmara: a new interpretation based on multi-channel seismic and multi-beam bathymetry data. *Earth and Planetary Science Letters*, 186(2), 143-158.
- Jian, X., Zhu, S. 2015. Predictive deconvolution for attenuation of multiple reflections in the marine seismic data processing. *Journal of Coastal Research* 73 (sp1), 310-314.
- Kurt, H., Yücesoy, E. 2009. Submarine structures in the Gulf of İzmit, based on multichannel seismic reflection and multibeam bathymetry. *Marine Geophysical Researches* 30(2), 73-84.
- Liu, J., Lu, W. 2008. An improved predictive deconvolution based on the maximization of Non-Gaussianity. *Applied Geophysics* 5(3), 189-196.

- Liu, L., Lu, W. 2014. Non-Gaussianity-based time-varying predictive deconvolution for multiple removals. Society Exploration Geophysicist Technical Program Expanded Abstracts, 4162-4166.
- Margrave, G. F., Lamoureaux, M. P. 2010. Nonstationary predictive deconvolution. CREWES Research, Report No: 21, 23.
- Marino, I. K., Santos, M. A. C., Silva, C. G. 2013. Processing of high-resolution, shallow seismic profiles, Guanabara Bay-Rio de Janeiro State, Brazil. *Revista Brasileira de Geofisica* 31(4), 579-594.
- Oğuz, S. 2012. Marmara Denizi orta sırtı ve Kumburgaz baseninde sıg gaz birikimlerinin sismik analizleri. Yüksek Lisans Tezi, Dokuz Eylül Üniversitesi, Fen Bilimleri Enstitüsü, 76 (unpublished).
- Peacock, K. L., Treitel, S. 1969. Predictive deconvolution: theory and practice. *Geophysics* 34(2), 155-169.
- Perez, M. A., Henley, D. C. 2000. Multiple attenuations via predictive deconvolution in the radial domain. CREWES Research, Report No: 12, 20.
- Perinçek, E. 2011. Tekirdağ Havzası yüksek çözünürlüklü sismik yansıma verilerinin işlenmesi ve yorumlanması. Yüksek Lisans Tezi, İstanbul Teknik Üniversitesi, Fen Bilimleri Enstitüsü, 95 (unpublished).
- Porsani, M. J., Ursin, B. 1998. Mixed-phase deconvolution. *Geophysics* 63(2), 637-647.
- Porsani, M. J., Ursin, B. 2007. Direct multichannel predictive deconvolution. *Geophysics* 72(2), H11-H27.
- Robinson, E. A. 1957. Predictive decomposition of seismic traces. *Geophysics* 22(4), 767-778.
- Robinson, E. A. 1967. Predictive decomposition of time series with application to seismic exploration. *Geophysics* 32(3), 418-484.
- Robinson, E. A. 1975. Dynamic predictive deconvolution. *Geophysical Prospecting* 23(4), 779-797.
- Schoenberger, M., Houston, L. M. 1998. Stationarity transformation of multiples to improve the performance of predictive deconvolution. *Geophysics* 63(2), 723-737.
- Shankar, U., Singh, S. S., Sain, K. 2009. Signal enhancement and multiple suppression using radon transform: an application to marine multichannel seismic data. *Marine Geophysical Researches* 30(2), 85-93.
- Sheng, C., Zhen, Z., Jun, G. 2014. A marine case analysis of multiple suppression. Beijing 2014 International Geophysical Conference and Exposition, 21 - 24 April 2014, Society of Exploration Geophysicists Global Meeting Abstracts, Beijing, China, 261-264.
- Sheriff, R. E., Geldart, L. P. 1995. *Exploration Seismology*. Cambridge University Press. 592.
- Sinton, J. B., Ward, R. W., Watkins, J. S. 1978. Suppression of long-delay multiple reflections by predictive deconvolution. *Geophysics* 43(7), 1352-1367.
- Şapaş, A. 2010. Investigation of rheological implications of the crustal reflectivity in the Sea of Marmara. PhD Thesis, İstanbul Technical University, Institute of Applied Sciences, 130 (unpublished).
- Taner, M. T. 1980. Long-period sea-floor multiples and their suppression. *Geophysical Prospecting* 28(1), 30-48.
- Taner, M. T., Coburn, K. W. 1981. Surface consistent estimation of source-and-receiver response functions, *Geophysics* 46(4), 412-413.
- Ulrych, T. J., Matsuoka, T. 1991. The output of predictive deconvolution. *Geophysics* 56(3), 371-377.
- Verschuur, D. J. 2013. *Seismic Multiple Removal Techniques: Past, Present, and Future*. European Association Geoscientists and Engineers Publications, Houten, Netherlands, 212.
- Wang, B., Cai, J., Guo, M., Mason, C., Gajawada, S., Epili, D. 2011. Postmigration multiple prediction and removal in the depth domain. *Geophysics* 76(5), WB217-WB223.
- Weglein, A. B. 1999. Multiple attenuations: an overview of recent advances and the road ahead. *The Leading Edge* 18(1), 40-44.
- Yuza, N. H., Nainggolan, T. B., Manik, H. M. 2019. Multiple attenuation methods in short-offset 2d marine seismic data: a case study in Cendrawasih Bay. Institute of Physics Conference Series: Earth and Environmental Science 429, 012031.
- Yücesoy, E. E. 2006. İzmit Körfezi Çok Kanallı Sismik Yansıma Verilerinin Değerlendirilmesi. Yüksek Lisans Tezi, İstanbul Teknik Üniversitesi, Fen Bilimleri Enstitüsü, 72 (unpublished).